Available online at www.sciencedirect.com
SCIENCE DIRECT®
Journal of Nuclear Materials 329–333 (2004) 248–251
journal of nuclear materials
www.elsevier.com/locate/jnucmat

Fatigue crack growth behavior of JLF-1 steel including TIG weldments

S.W. Kim [a,c,*], H.K. Yoon [a], W.J. Park [b], A. Kohyama [c]

[a] Department of Mechanical Engineering, Dong-Eui University, 24, Gaya Dong, Pusan Jin-Gu, Pusan 614-714, South Korea
[b] Department of Mechanical and Ship Engineering, Gyeongsang National University, 445, In-Pyeng Dong, Tongyeong, Gyeongnam 650-160, South Korea
[c] Institute of Advanced Energy, Kyoto University, Gokasho, Uji, Kyoto 611-0011, Japan

Abstract

The fatigue crack growth behavior of JLF-1 steel is very important for estimating life in terms of a critical crack length in a blanket. As a part of this work, the fatigue crack growth behavior of JLF-1 steel was examined in terms of the fatigue crack growth rate (da/dN) versus the stress intensity factor range (ΔK) curves. Test specimens consisted of full size compact tension (FCT) and half size compact tension (HCT) specimens of the base metal and TIG welded metal. The fatigue crack growth testing was carried out at constant amplitude cyclic loading under a stress ratio of 0.3 at RT and 673 K. From these results, the effects of TIG welding, test temperature and specimen size on fatigue crack growth behaviors are discussed within the Paris region. The fracture mechanisms of the fatigue crack growth test specimens were also analyzed using scanning electron microscopy (SEM).

1. Introduction

Nuclear fusion energy reactors not only need high efficiency of energy production but also development of structural materials that allow efficient operation. The candidate blanket structural materials for nuclear fusion reactors may be RAFs, vanadium alloys and SiC/SiC composite etc. in accordance with cooling system chosen [1,2]. RAFs is particularly suited for nuclear fusion reactors because of a low coefficient of thermal expansion and excellent heat conductivity. Recently, development and testing has been carried out for F82H and JLF-1 steels developed by the JAERI and JUPITER programs, respectively [3,4]. Kohyama et al. and Hasegawa et al. [5,6]. employed 9–12 wt%Cr for Fe–Cr–W RAFs in order to obtain excellent high temperature strength under 873 K comparable to austenitic heat resisting steel (SUS 304 or 316). Evaluation of EB welding (electron beam welding) and TIG welding (tungsten inert gas arc welding) weldment properties is an important issue because of welding is necessary for production of nuclear fusion reactors [7,8].

In this work, the fatigue crack growth (FCG) behavior of JLF-1 steel was examined to construct database for fatigue crack growth rate (FCGR; da/dN) versus stress intensity factor range (ΔK). The FCG test was carried out by constant amplitude cyclic load testing under a stress ratio of 0.3 at RT and 673 K using full size compact tension (FCT) and half size compact tension (HCT) specimens of base metal and TIG weldments. The effects of TIG weld, test temperature and specimen size on FCG behaviors are discussed within the Paris region. Also, the fracture mechanisms for FCG are analyzed using scanning electron microscopy (SEM).

2. Experimental procedure

The 25 mm thick plate was normalized at 1323 K for 1 h and air cooled, then tempered at 1050 K for 1 h

* Corresponding author. Address: Department of Mechanical Engineering, Dong-Eui University, 24, Gaya Dong, Pusan Jin-Gu, Pusan 614-714, South Korea. Tel.: +81-774 38 3466; fax: +81-774 38 3467.
E-mail address: kimsw@iae.kyoto-u.ac.jp (S.W. Kim).

0022-3115/$ - see front matter © 2004 Elsevier B.V. All rights reserved.
doi:10.1016/j.jnucmat.2004.04.019

followed by air cooling. Two plates were butt-welded by TIG welding process after preparing a U-shaped groove. Post welding heat treatment was performed at 1013 K for 3 h followed by furnace cooling. TIG welding conditions and a schematic diagram of the U-shape groove are shown in Table 1 and Fig. 1, respectively. The chemical composition of the JLF-1 steel is shown in Table 2. Also, Fig. 2 shows the micro Vickers hardness distribution of the cross section of the TIG weld joint. The hardness of weld metal (WM) was higher than that of the base metal by about 20%, and lowest hardness point appeared at the interface between the base metal and the heat affected zone (HAZ).

Table 3 shows the mechanical properties of JLF-1 steel. The WM specimen has higher strength and lower elongation than other test specimens at RT. In the case of the weld metal of transverse direction to welding direction, the test specimen was fractured within the interface between base metal and HAZ. Therefore, tensile properties of the weld metal of transverse direction specimen can be regarded as a result of HAZ. As these results, the tensile strength of JLF-1 steel increased in the order of HAZ, base metal and weld metal. Also, total elongation increased in the order of HAZ, weld metal and base metal.

All of the tests were carried out using a computer controlled electro-servo hydraulic testing machine (MTS model 810, 10tonf). The FCG tests were performed under a constant amplitude cyclic loading mode at RT and 673 K. The wave form was sinusoidal with a frequency of 10 Hz and stress ratio of 0.3. The fatigue crack length was measured by a compliance method using a crack opening displacement (COD) gage and was observed by traveling optical microscope with resolution of 0.001 mm. The shape and dimensions of CT specimens for FCG tests is presented in Fig. 3. In the case of weld metal specimens, the welding direction is same with the fatigue cracking direction.

Table 1
TIG welding condition

Current	230–250 A
Voltage	10.5 V
Travel speed	10 cm/min
Heat input	14.5–15.8 kJ/cm
Preheat temperature	$\leqslant$473 K
Interlayer temperature	$\leqslant$473 K
Number of passes	$\sim$20
Wire diameter	1.2 mm

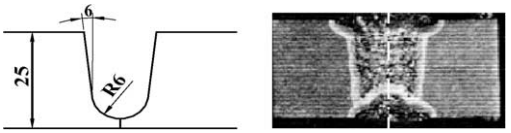

Fig. 1. U-groove shape and microstructure.

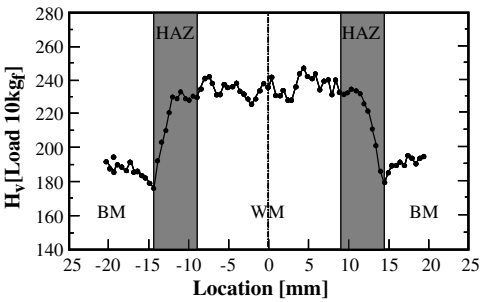

Fig. 2. Hardness distribution after TIG welding.

Table 2
Chemical composition of base metal, weld metal and welding wire

	C	Si	Mn	P	S	Al	Cr	W	V	Ta	N	Ti	B
BM	0.10	0.05	0.45	0.003	0.002	0.003	8.85	1.99	0.20	0.08	0.0231	–	0.0002
WM	0.061	0.13	0.43	0.005	0.003	0.003	9.16	1.91	0.25	0.081	0.0259	0.019	0.0001
WW	0.061	0.10	0.45	0.003	0.003	0.002	8.96	1.82	0.25	0.084	0.0332	0.028	0.0001

BM: Base metal, WM: weld metal, WW: welding wire.

Table 3
Mechanical properties of JLF-1 steel

Material	Test temperature (K)	Yield strength (MPa)	Tensile strength (MPa)	Elongation (%)
Base metal	RT	449	612	28.1
	673 K	–	531	25.4
Weld metal	RT	630	733	24.5
	673 K	–	663	21.4

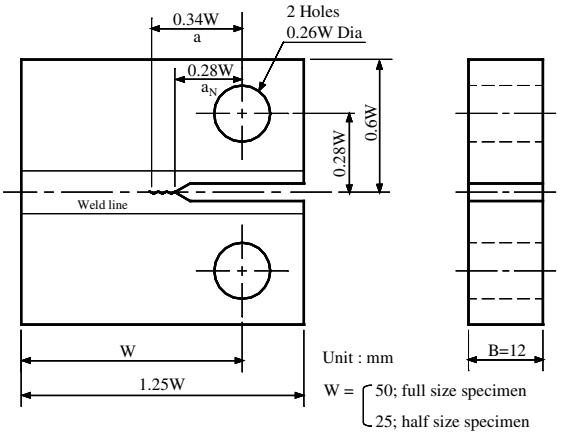

Fig. 3. Dimensions of CT specimens for FCG tests.

3. Results and discussion

3.1. FCG behavior

FCG behavior is generally characterized using linear elastic fracture mechanics (LCFM) principles, and FCG curves are divided into regions I, II and III. The FCGRs in the subcritical region II is related to the stress intensity factor range as follows (Paris law):

$$da/dN = C(\Delta K)^m,$$

where C and m are material constants.

The FCGRs of base metal and welded metal of JLF-1 steel are summarized using an incremental polynomial method as shown in Fig. 4(a) and (b). Those plots show the region II results with the Paris law parameters. The FCGRs of base metal and welded metal at 673 K are slightly faster than those at RT due to a decrease in tensile strength and elongation. Generally, the FCGRs are inversely proportion to the strength of material. Those results are in good agreement with other published data for RAFs [9].

The FCGRs of half size specimens are almost the same as those of full size specimens. Therefore, it is believed that the specimen size little affects the FCGRs for JLF-1 steel at RT. Although it is still necessary to perform an evaluation of crack closure and fracture mechanics, it is expected that the FCG behavior of JLF-1 steel can be evaluated by using small sized specimens at RT.

Comparing (a) and (b), the FCGRs for weld metal are almost the same with those of base metal without regard to test temperature and test specimen size. In the case of similar alloys, the FCGRs of weld metal is faster than that of base metal [10].

3.2. Fracture mechanism

Fig. 5 shows the fracture surface of FCG test specimens using SEM to evaluate the fracture mechanisms. Each figure shows region II ($\Delta K = 27$ MPa m$^{1/2}$). In

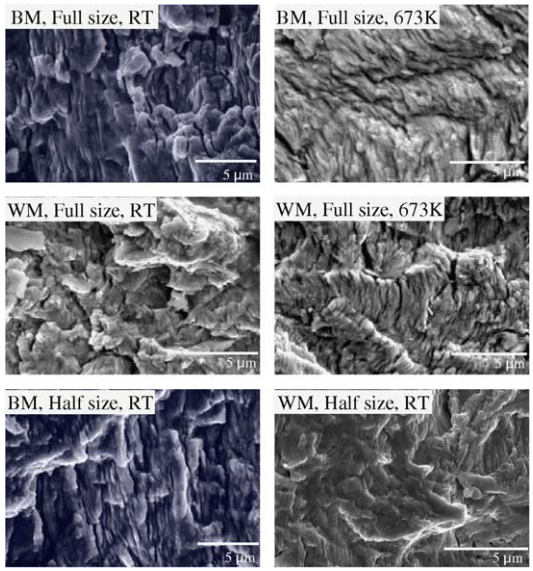

Fig. 5. SEM fractographs of JLF-1 steel at $\Delta K = 27$ MPa m$^{1/2}$.

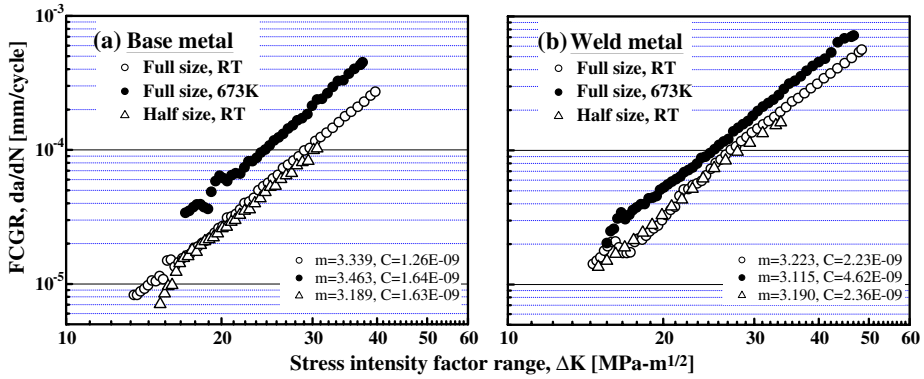

Fig. 4. Results of FCG tests for (a) base metal and (b) weld metal of JLF-1 steel.

these figures, the fracture surface of the FCG test specimen shows very fine fatigue striations on some of facets indicating the presence of extremely localized plasticity deformation. In the case of weld metal, there are considerable quasicleavage fracture surfaces mainly to small precipitates from the welding process at RT.

4. Conclusion

1. The FCGRs of base metal and weld metal at 673 K are slightly faster than those at RT due to a decrease in tensile strength and elongation.

2. Specimen size dose not affect the FCGRs of JLF-1 steel at RT. Therefore, the FCG behaviors of JLF-1 steel can be evaluated by using small sized specimens.

3. The FCGRs of weld metal are almost the same as those of base metal without regard to test temperature and test specimen size.

4. SEM fractography of the FCG test specimen shows very fine fatigue striation on some of facets indicating the presence of very localized plastic deformation. In the case of weld metal, there is considerable quasicleavage fracture surface mainly to small precipitates from the welding process at RT.

Acknowledgements

This study is supported by Invitation Fellowship for the Long-term Research Program in Japan Society for the Promotion of Science (JSPS). The authors wish to thank the persons concerned.

References

[1] K. Shiba, M. Suzuki, A. Hishinuma, J. Nucl. Mater. 233–237 (1996) 309.
[2] A. Kohyama, H. Matsui, A. Hishinuma, Proc. of 10th Pacific Basin Nucl. Conf. (1996) 883.
[3] S. Jitsukawa, M. Tamura, B. van der Schaaf, R.L. Klueh, A. Alamo, C. Petersen, M. Schirra, P. Spaetig, G.R. Odette, A.A. Tavssoli, K. Shiba, A. Kohyama, A. Kimura, J. Nucl. Mater. 307–311 (2002) 179.
[4] Y. Kohno, Annual Progress Report of Japan/US Collaborative Research Utilizing the FFTF/MOTA, 1987, p. 73.
[5] A. Kohyama, Y. Kohno, K. Asakura, H. Kauano, J. Nucl. Mater. 212–215 (1994) 684;
A. Kohyama, Y. Kohno, M. Kuroda, A. Kimura, F. Wan, J. Nucl. Mater. 258–263 (1998) 1319.
[6] T. Hasegawa, Y. Tomita, A. Kohyama, J. Nucl. Mater. 258–263 (1998) 1153.
[7] N. Inoue, T. Muroga, A. Nishimura, T. Nagasaka, O. Motojima, S. Uchida, H. Yabe, K. Oguri, Y. Nishi, Y. Katoh, A. Kohyama, J. Nucl. Mater. 283–287 (2000) 1187.
[8] N. Inoue, T. Muroga, A. Nishimura, O. Motojima, J. Nucl. Mater. 258–263 (1998) 1248.
[9] L.A. James, K.W. Carlsen, J. Pressure Vessel Technol. 107 (1985) 271.
[10] H. Nishi, M. Eto, K. Tachibana, K. Koizumi, M. Kakahira, H. Takagashi, J. Eng. Des. 58 (2001) 869.